Colloids and Surfaces B: Biointerfaces 122 (2014) 175–183

Contents lists available at ScienceDirect

Colloids and Surfaces B: Biointerfaces

journal homepage: www.elsevier.com/locate/colsurfb

Biodegradable gelatin–ciprofloxacin–montmorillonite composite hydrogels for controlled drug release and wound dressing application

Bhavesh D. Kevadiya[a,b,1,2], Shalini Rajkumar[b,2], Hari C. Bajaj[a,*], Shiva Shankaran Chettiar[c,3], Kalpeshgiri Gosai[a,1], Harshad Brahmbhatt[a,1], Adarsh S. Bhatt[a,1], Yogesh K. Barvaliya[d], Gaurav S. Dave[d], Ramesh K. Kothari[e,4]

[a] Discipline of Inorganic Materials and Catalysis, Central Salt and Marine Chemicals Research Institute, Council of Scientific and Industrial Research (CSIR), Gijubhai Badheka Marg, Bhavnagar 364 021, Gujarat, India
[b] Institute of Science, Nirma University, Ahmedabad 382 481, Gujarat, India
[c] Department of Biotechnology, Shree Ramkrishna Institute of Computer Education and Applied Sciences, Veer Narmad South Gujarat University, Surat, India
[d] Department of Biochemistry, Saurashtra University, Rajkot 360 005, Gujarat, India
[e] Department of Microbiology, Christ College, Rajkot 360 005, Gujarat, India

ARTICLE INFO

Article history:
Received 15 February 2014
Received in revised form 21 June 2014
Accepted 23 June 2014
Available online 30 June 2014

Keywords:
Biodegradation
Cell migration
Ciprofloxacin
Montmorillonite
Wound healing

ABSTRACT

This work reports intercalation of a sparingly soluble antibiotic (ciprofloxacin) into layered nanostructure silicate, montmorillonite (MMT) and its reaction with bone derived polypeptide, gelatin that yields three-dimensional composite hydrogel. Drug intercalation results in changes in MMT layered space and drug loaded MMT and gelatin creates 3D morphology with biodegradable composite hydrogels. These changes can be correlated with electrostatic interactions between the drug, MMT and the gelatin polypeptides as confirmed by X-ray diffraction patterns, thermal, spectroscopic analyses, computational modeling and 3D morphology revealed by SEM and TEM analysis. No significant changes in structural and functional properties of drug was found after intercalation in MMT layers and composite hydrogels. *In vitro* drug release profiles showed controlled release up to 150 h. The drug loaded composite hydrogels were tested on lung cancer cells (A549) by MTT assay. The results of *in vitro* cell migration and proliferation assay were promising as composite hydrogels induced wound healing progression. *In vitro* biodegradation was studied using proteolytic enzymes (lysozyme and protease K) at physiological conditions. This new approach of drug intercalation into the layered nanostructure silicate by ion-exchange may have significant applications in cost-effective wound dressing biomaterial with antimicrobial property.

1. Introduction

Tissue engineering is a speedily budding area of medical sciences, which generally requires use of special biodegradable and biocompatible, cost-effective, antimicrobial materials for topical applications such as wound dressings [1–3]. Tissue cell restorations at the site of the wound are often vulnerable to bacterial infection, which can be forbidden by antimicrobial drugs loaded on composite nanomaterials for controlled drug release. Various approaches that exist to deter bacterial growth include the use of nanoparticles [4–9] for sustained release of antibiotics at the specific site of application [10–13]. Ciprofloxacin (CPX) (fluoroquinolone, 1-cyclopropyl-6-fluoro-4-oxo-7-(piperazin-1-yl)-1,4-dihydroquinoline-3-carboxylicacid hydrochloride) is one of the most efficient antimicrobials used for a variety of topical applications, such as skin, eye, nose and ear infections. A drug formulation must deliver required concentration of the drug in a sustained manner at specific locations. In order to address these requirements, formulations such as polymers, polymeric/gel *e.g.* carbopol gel, lactic acid, hydroxyl propyl methyl cellulose and layered double hydroxides are usually employed, as they offer superior vehicles for the integration of drug and controlled release property [13–19].

Abbreviations: MMT, montmorillonite/Na^+-clay; TEM, transmission electron microscopy; XRD, X-ray diffraction; SEM, scanning electron microscopy; CPX, ciprofloxacin; Gel, gelatin.

* Corresponding author. Tel.: +91 278 2471793; fax: +91 278 2567562.
E-mail addresses: shalini.rjk@nirmauni.ac.in (S. Rajkumar), hcbajaj@csmcri.org, hcbajaj13@rediffmail.com (H.C. Bajaj), scheti@gmail.com (S.S. Chettiar), yogeshbaravalia@yahoo.in (Y.K. Barvaliya), kothari1971@gmail.com (R.K. Kothari).
[1] Tel.: +91 278 2471793; fax: +91 278 2567562.
[2] Tel.: +91 2717 241900–04/241911–15; fax: +91 2717 241916/17.
[3] Tel.: +91 0261 2240172; fax: +91 0261 2240170.
[4] Tel.: +91 281 2587901/3; fax: +91 281 2570301.

http://dx.doi.org/10.1016/j.colsurfb.2014.06.051
0927-7765/

However, there are also imperative boundaries such as undesired release patterns of drugs, need for repeated dosing, biodegradation issue, low stability of drug, solvent base casting/formulation and costly synthetic materials, long time duration for material preparation with complex fabrication procedure and toxicity of unreacted synthetic polymer precursors that need to be addressed.

During the past few years, layered silicate-biopolymer based nanomaterials with the advantages of ion exchange competence, drug load potentiality and prospect of tuning physicochemical properties (such as chemical modification, porosity, and mechanical potency) to match normal body tissue, load drug molecules for controlled release at specified site and production of scaffolds for tissue engineering have been explored [1,20–30]. Gelatins are protein biopolymers derived from collagenous animal tissues by controlled hydrolysis [31,32]. It can be visualized as a copolymer build up from triads of α-aminoacids with glycine (gly) at every third position (soft blocks) and triads of hydroxyproline (hypro), proline (pro) and glycine (rigid blocks), with a narrow molar mass distribution [33]. Because of many merits, such as biological origin, biodegradability, biocompatibility and commercial availability at relatively low cost, gelatin has been widely used in biomedical applications [34]. In pharmaceutical and medical fields, gelatin has long been used as a sealant for vascular prostheses [35–37], carrier for drug delivery [38], wound healing dressings [39], parts of biomedical tools and surgical objects, *etc*. Medical clay (montmorillonite, MMT) on the other hand is naturally abundant and has null toxicity, drug loading capability and mucoadhesiveness. It also has potential to adsorb dietary toxins, bacterial toxins associated with gastric turbulences, hydrogen ions in acidosis and metabolic toxins such as steroidal metabolites associated with pregnancy [20–29]. Gel/MMT composites show excellent cell affinity, biocompatibility, promote cell proliferation and migration, controllable biodegradation and superior mechanical properties [1,29,34,40–43].

Keeping this in view this study was aimed to characterize a biofunctional, composite hydrogel material in terms of structure and morphological properties in order to obtain applicable composite hydrogel for wound healing and external usage with controlled releases of antibacterial drug (CPX) for preventing microbial infections. Our first aim was focused on preparing CPX loaded montmorillonite (CPX–MMT) which was further modified with gelatin (gel) to form MMT–gel composite hydrogels with prospective application at tissue engineering (wound healing) and controlled release of broad spectrum antimicrobial. Our second aim was to evaluate effects of composite hydrogels on inhibition of cell growth, cell proliferation and migration. Our last aim was to determine if the entrapped drug could be released in a controlled manner and to determine effect of proteolytic enzymes on biodegradation of composite hydrogels. Unique characteristics of composite hydrogels like controlled release pattern, biodegradation, cell proliferation and biocompatibility make it a potential applicant for wound healing applications.

2. Experimental

2.1. Materials

For the present study, a bone gelatin (type-b) was gifted from Raymon Patel Gelatine Pvt. Ltd. Vasad (India). Ciprofloxacin (CPX) and sodium MMT (Closite Na^+) were gifted from Corel Pharma Pvt. Ltd. (India) and southern clay products incorporation, USA, respectively. Cellulose acetate dialysis tube (cutoff MW: 7014 Da) and proteinase-k were purchased from Sigma–Aldrich, USA. RPMI-1640 (Roswell Park Memorial Institute 1640), trypan blue, MTT (3-(4,5-dimethylthiazole-2-yl)-2,5-diphenyl tetrazolium bromide), trypsin, streptomycin sulfate, penicillin, amphotericin, fetal calf serum (FCS), lysozyme (5×10^4 U/ml) and DMSO were procured from himedia laboratory, India. HPLC grade methanol, acetonitrile and analytical grade potassium di-hydrogen phosphate, phosphoric acid, EDTA was purchased from S.D. Fine Chemicals Pvt. Ltd. Millipore water was prepared by a Milli-Q plus system (Millipore Corporation, USA).

2.2. CPX–MMT hybrid preparation

Intercalation of CPX in MMT interlayer gallery was carried out by batch technique. For this purpose, 1 g of MMT was mixed with 100 ml of aqueous drug solutions (1 g of CPX with pH = 3.5) and stirred (800 rpm) for 24 h, filtered, washed several times with water to remove the non-intercalated CPX, dried at 60 °C and ground with mortar and pestle to obtain a fine powder [20–24,28]. This sample was designated as CPX–MMT hybrid. The remaining concentrations of CPX in the filtrates were measured by UV absorbance at λ_{max} = 270 nm. The entire intercalation studies were performed in triplicates and the values were averaged for data analysis.

2.3. Preparation of CPX–MMT–gel composite hydrogels

CPX–MMT–gel composite hydrogels were prepared by simple gelling method and freeze-drying technique. 10% (*w*/*v*) of gelatin was dispersed in warm water under vigorous stirring to prepare a viscous solution. The CPX–MMT hybrid was added in the optimized mass ratio CPX–MMT to gelatin of 1:1.33 (% *w*/*w*) under continuous stirring. The mixture was stirred for 5 h to obtain complete homogenous composite hydrogels. Then the composite hydrogel solutions were poured into plastic molds and kept at −2 °C for 24 h to solidify. After solidification, they were subsequently cut into small cubes (∼0.5 cm) and rapidly frozen at −80 °C and freeze-dried (Virtis Bench-Top-K, Virtis Co., Gardiner, USA). Similar methods were followed for preparation of composite hydrogels without drug and pristine gelatin hydrogels with drug. The outline of the composite hydrogel preparation is graphically represented (supplementary data: S1).

2.4. Characterization

All the samples were characterized by powder X-ray diffraction (XRD) (Miniflex-II desktop X-ray diffractometer, Rigaku, Japan) with the curved Ni-filtered CuKα (λ = 1.5418) radiation with a scanning of 1°/min in 2θ range of 2–80°. Fourier transform infrared spectra (FT-IR) were recorded on Perkin–Elmer, GX-FT-IR as KBr pellet over the range 4000–400 cm^{-1}. Thermo gravimetric analysis (TGA) was carried out within 30–800 °C at the heating rate of 10 °C/min under nitrogen flow (20 ml/min) using TGA/SDTA 851e, Mettler-Toledo, Switzerland. Differential scanning calorimetric (DSC) studies were carried out in the range of 30–400 °C at the heating rate 10 °C/min under nitrogen flow (10 ml/min) using Mettler-Toledo, DSC-822e, Switzerland. The surface morphology of composite hydrogels was observed in scanning electron microscope (SEM), LEO-1430VP, UK. Internal morphology of the CPX–MMT hybrid and CPX–MMT–gel composite hydrogels were observed using a JEM-2100 transmission electron microscope (TEM) (JEOL, Tokyo, Japan), with an accelerating voltage of 200 kV. The sample was prepared in Milli-Q water and dried on a copper grid at room temperature and images were taken under bright-field condition with exposure times of 2 Ys. The UV–visible absorbance of drug solutions were measured at λ_{max} = 270 nm using UV–visible spectrophotometer UV2550 (Shimadzu, Japan), equipped with a quartz cell having a path length of 1 cm.

2.5. Cell culture experiments

2.5.1. Cell culture

A549 (Human lung adenocarcinoma epithelial cell line) was obtained from National Repository of Animal Cell Culture, National Center for Cell Sciences (NCCS), Pune, India. A549 cells were grown in 12 well cell culture plate (Tarson–980020, 12 well plates; Tarson India) in RPMI 1640, supplemented with 10% fetal calf serum (FCS), 100 μg/ml of streptomycin sulfate, 0.25 μg/ml of amphotericin, 100 U/ml of penicillin incubated under 5% CO_2 at 37 °C (N-Biotek NB203XL, Korea). Cells were trypsinized from parent stock of 9th passage and subjected to viability and total count. Cells were resuspended in fresh media to make dilution of 2×10^3 cells/well. Cells were grown to achieve more than 80% confluence (which was achieved normally by 48 h) and further cells were exposed to pristine drug, drug carriers and drug loaded composite hydrogels along with media change for duration of 24 h. Concentration and duration of the test formulations were selected based on the preliminary metabolic stress indices monitored by MTT assay.

2.5.2. Exposure to composite hydrogels (MTT assay [44])

The stock solutions were prepared by addition of CPX–MMT, CPX–MMT–gel and CPX–gel (10 mg/ml equivalent of CPX) in Milli-Q water and sterilized by syringe filtration with 0.22 μm pore size filter (Whattmann Filters). Cells were cultured in wells designated according to the dose addition. Culture wells were designated as group one to seven: G1: control, G2: pristine CPX, G3: pristine MMT, G4: pristine gelatin, G5: MMT–gel, G6: CPX–gel and G7: CPX–MMT–gel, while wells were also run with only media, carriers with media and composite hydrogel formulations to monitor contamination from either sources. Cells not treated with any xenobiotic served as experimental controls. CPX and formulated composite hydrogels were exposed to cells at variable concentrations of 10, 50, 100 and 200 mg/ml (equivalent of CPX). Carrier materials (G3–G5) were added to cultures to match the total exposure as in composite hydrogels and all groups were exposed for 24 h.

Media from control and experimental cultures exposed to composite hydrogels were aspired out and washed with sterile phosphate buffered saline (PBS) couple of times to remove any traces of test composites in culture. 100 μl of MTT (3-(4,5-dimethylthiazol-2-yl)-2,5-diphenyltetrazolium bromide) dye (5 mg/ml PBS) was added to each well and further incubated for 4 h in same physical conditions. After the incubation period the cultures were gently shaken and media with excess non reacted dye was removed and 1 ml of DMSO was added to the cells, so as to solublize the colored formazan formed. The absorbance was measured using spectrophotometer (Systronics-2201 Digital spectrophotometer, India) at λ_{max} = 490 nm against running DMSO as blank. The percentage growth inhibition was calculated using the formula below:

$$\text{Cell inhibition}\,(\%) = 100 - \left\{\frac{At - Ab}{Ac - Ab}\right\} \times 100 \quad (1)$$

where *At* is the absorbance value of test formulation, *Ab* is the absorbance value of blank and *Ac* is the absorbance value of control.

2.6. In vitro biodegradation assay

The *in vitro* biodegradation of composite hydrogels was carried out in phosphate buffered saline (PBS). The initial weight of freeze-dried composite hydrogel cubes was recorded prior to immersing in phosphate buffered saline (PBS) [1]. The composite hydrogel cubes were then treated with lysozyme (5×10^4 U/ml) and proteinase K (10 μg/ml) at 37 °C in sterile incubation tube. Samples were collected from the incubation tube rinsed thoroughly with distilled water and vacuum dried to avail their dry weight. Specimens were collected at regular interval of 24 h and degradation percentage was calculated. The degradation percentage *D* was determined by the following weight equation:

$$D\,(\%) = \frac{W_0 - W_t}{W_0} \times 100 \quad (2)$$

where W_0 represented the initial weight, while W_t was the weight at time "*t*". The degradation percentage *D* was expressed as the mean ± standard deviation.

2.7. Monolayer wound healing assay (migration assay)

Cells were stimulated to migrate in response to composite hydrogels in wound healing by *in vitro* cell migration assay [45]. A549 cells were cultured and brought to confluence in 12 well culture plates for migration assay. Migration assay was carried out by scratch wound-healing method, where the wound was instigated by gently scratching the base of the well by a micropipette tip. Clear margin of the area with central cell free zone was confirmed under an inverted microscope (CKX Inverted microscope, Olympus, India), then each well was rinsed using sterile phosphate buffered saline (PBS) and media with different formulated composite hydrogels were added to respective wells. The plates were incubated at 37 °C, 5% CO_2 for 24 h. The number of cells that had migrated from the edge of the wound in each 250 μm × 500 μm area of 10 randomly chosen fields was counted. Results were expressed as the average number of cells per field.

2.7.1. In vitro release behavior of CPX

In vitro CPX release studies were carried out in 0.1 M phosphate buffered media of pH 7.4 using the dialysis bag technique [20–24]. Dialysis bags were equilibrated with dissolution medium for a few hours prior to experiments. The weighed quantities of pristine CPX, CPX–MMT and CPX–MMT–gel (equivalent to 10 mg of entrapped CPX) were suspended in dialysis bag containing 5 ml of release medium. Dialysis bag was dipped into the receptor compartment containing 100 ml dissolution medium, which was shaken at 37 ± 0.5 °C in Julabo shaking water bath (SW23) at 100 rpm. 1 ml aliquots were withdrawn at regular time interval and the same volume was restored with the fresh release medium. Samples were analyzed by high-performance liquid chromatography (HPLC) performed in triplicates and the average values were used in the data analysis.

2.7.2. CPX quantification by HPLC

The quantification of CPX in release medium was determined using a validated HPLC method reported in literature with slight modifications [46]. Briefly, consequent to preparation of CPX standard in the mobile phase, analysis by HPLC system consisting of photodiode array detector (Waters Alliance model: 2695 separation module with Waters-2996 Photodiode Array Detector, Waters Corporation, Milford, MA, USA) and Enable C18H column (Shimadzu HPLC column with length = 15 cm, ID = 4.6 mm, particle size = 5.0 μm, Shimadzu Corporation, Kyoto, Japan) was carried out. CPX containing release medium samples were transferred to auto sampler vials, capped and placed in cassettes of the HPLC auto sampler. Mobile phase employed for analysis was mixture of acetonitrile:water containing 0.25 M H_3PO_4 (60:40, v/v). The injection volume was 20 μl and retention time of CPX was found to be 5 min. The detection wavelength (λ_{max}) for CPX was 275 nm and CPX concentration in release medium was determined using the standard curve obtained for known concentrations of CPX in mobile phase processed under identical conditions. The curve was found to be linear with a R^2 = 0.9948.

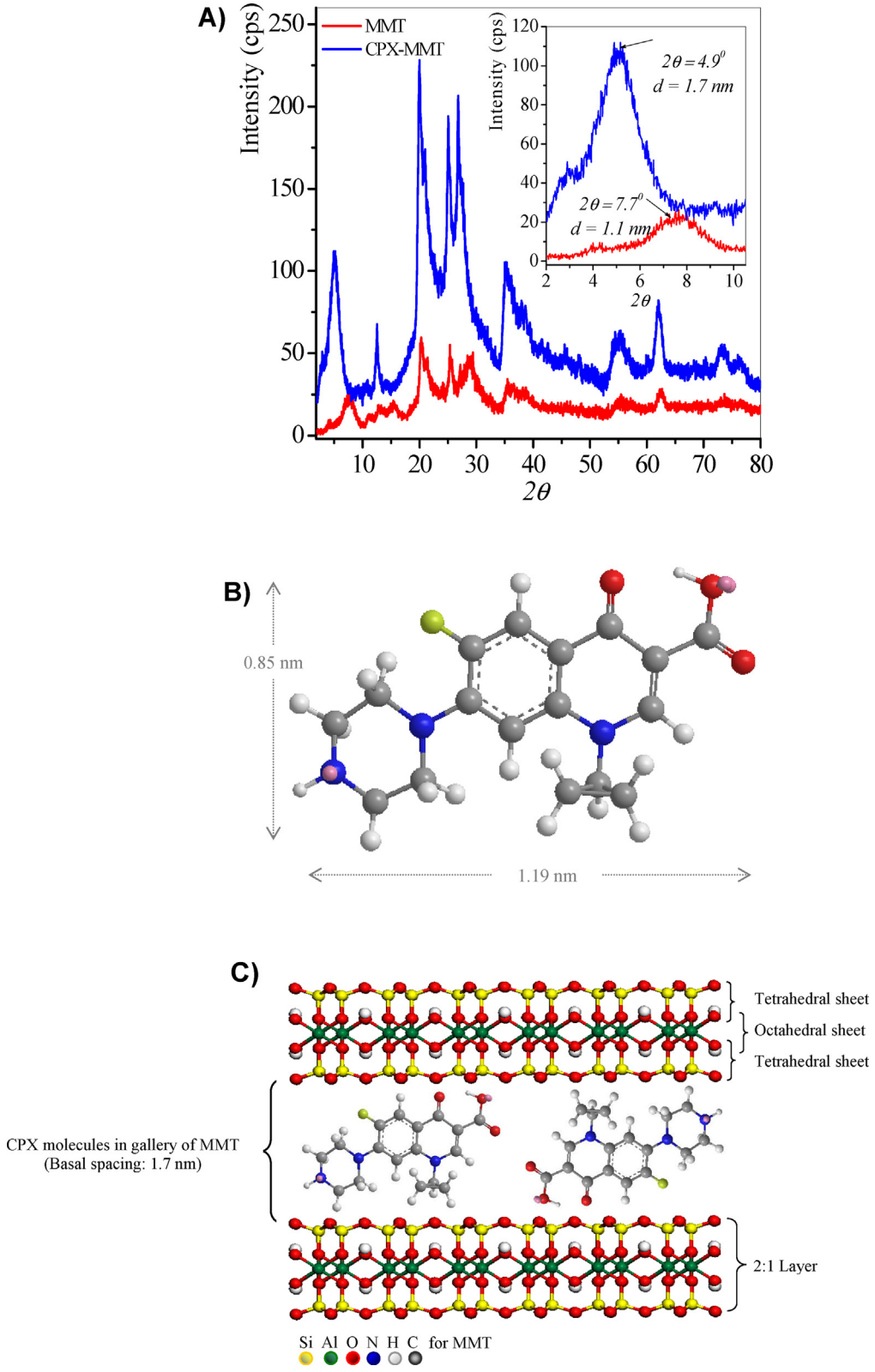

Fig. 1. (a) XRD patterns of pristine MMT and CPX–MMT, (b) three dimensional molecular structures of CPX and (c) schematic illustration of CPX–MMT hybrid, showing CPX arrangement in the longitudinal monolayer mode in MMT gallery.

2.8. Statistical analysis

The quantitative proliferation of A549 cells under influence of different formulations was compared using one-way ANOVA. The values are presented as mean ± standard deviation and a difference of $p < 0.05$ was considered as significant. The statistical analysis was performed using Origin 8.0.

3. Results and discussion

3.1. Confirmation of ciprofloxacin intercalation in montmorillonite

3.1.1. X-ray diffraction and FT-IR analysis

The XRD patterns of pristine MMT and CPX intercalated MMT are illustrated in Fig. 1(a). MMT reflection at $2\theta = 7.7^\circ$ indicated basal spacing of 1.1 nm, whereas a major shifting of $2\theta = 7.7^\circ$ to $2\theta = 4.9^\circ$ with expansion of basal spacing up to 1.7 nm was observed in the case of CPX–MMT (containing 35.5% of CPX). The increased basal spacing after reaction of CPX with MMT was evidence of CPX intercalation into MMT. As the thickness of MMT sheet was 0.96 nm [21], the interlayer space height of CPX–MMT hybrid could be estimated to be 0.74 nm. This was marginally smaller than theoretical estimated value of longitudinal molecular length of CPX (0.85 nm) (ChemBio3D Ultra 11.0, Fig. 1(b)) while the lateral length of CPX molecule was 1.19 nm. It was presumed from the interlayer space height that the CPX molecules might have compressed during intercalation by electrostatic interaction in MMT (Fig. 1(c)). However, the intensity of the XRD characteristic peak increased in CPX–MMT, which indicated an impervious ordering of sheet structure caused by the cation exchange and higher restoration of charge density during drug loading. These results were close to our previous results of drug intercalation by ion exchange method [20–24,47,48]. In MMT structure, atoms within single layers strongly bond with each other, but the adjoining layers of MMT are stacked by weak dipolar or van der waals forces, leading to intercalation of water or polar organic molecules and causing the crystal lattice to expand in the *c* direction. The defection of the crystal lattice and the isomorphous substitution of alkaline or alkaline earth cations in the interlayer gap stimulate various layer charge, which are not homogeneously disseminated with respect to the interlayer space for cation-exchange [20–24,47,48]. As a result, interstratification occurs with unequally spaced silicate inter layers due to contradictory quantity of hydration. Consequently, some of the silicate layers were strongly bound to each other, not permitting CPX cations to penetrate in the MMT layer. On the other hand, the silicate layers, which were weakly bound to each other, allowed CPX cations to enter into the interlayer gallery of MMT [23].

FT-IR spectra of the CPX, CPX–MMT, CPX–MMT–gel composite hydrogels (containing 13.8% of CPX) and CPX–gel are shown in Fig. 2. The spectrum of MMT revealed characteristic absorption bands [20–24]. The pristine CPX had peak at 3380 cm^{-1} which corresponded to —NH stretching and peaks corresponding to —COOH indicated dimerization of drug in the range of 2460–3090 cm^{-1}. Dimerization is characteristic of acid functional group and occurs in the case of self-association in the drug molecule through weak van der waals forces [49]. The peaks at 2922 and 2840 cm^{-1} show aliphatic C—H stretching. The peak at 3088 cm^{-1} shows stretching of —COOH and 3525 cm^{-1} was due to —OH stretching, which was within standard range of 3400–3600 cm^{-1} peaks. The —C=O peak at 1700 cm^{-1} and quinolone peak was recorded at 1615 cm^{-1}. A strong absorption peak between 1022 cm^{-1} and 1000 cm^{-1} was assigned to —C—F group of CPX [50–52]. The CPX–MMT hybrid showed absorption bands at 3433 cm^{-1} due to —OH stretching band for adsorbed water in MMT. The shift in the band from

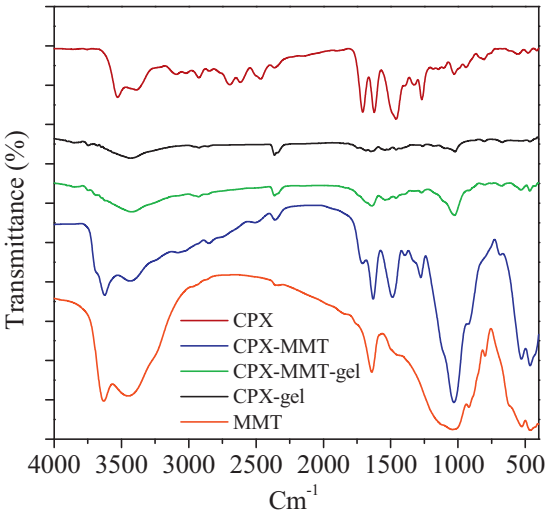

Fig. 2. FT-IR pattern.

3620 to 3632 cm^{-1} was due to —OH band stretching of Al—OH and Si—OH throughout interaction of CPX and overlaid absorption peak at 1630 cm^{-1} was attributed to —OH bending of adsorbed water in MMT. The peak at 2847 shows aliphatic —C—H stretching and presence of CPX in interlayer gallery of MMT was indicated by peak —C=O group at 1700 cm^{-1}. A strong absorption peak between 1026 cm^{-1} was assigned to C—F group of CPX. The existence of an amide I (—C=O stretching) at 1635 cm^{-1} indicated that CPX–gel/CPX–MMT–gel adopted predominantly α-helical configuration and this was confirmed by appearance of amide II at 1538 cm^{-1} (—NH bending and —CN stretching modes) [53]. Amide III (around 1270 cm^{-1}) band was somewhat complex, consisting of components from —CN stretching and —NH in plane bending from amide linkages, as well as absorptions arising from wagging vibrations from $-CH_2$ groups from the glycine backbone and proline side-chains [54]. The CPX–MMT–gel spectra illustrate that the Si—O—Si bonds of CPX–MMT shifted in the range of 1000–1500 cm^{-1}. The characteristic peaks of MMT shifted from 1491 cm^{-1} to 1480 cm^{-1}, from 1375 cm^{-1} to 1397 cm^{-1} and from 1030 cm^{-1} to 1026 cm^{-1}. This indicated hydrogen bonding interactions between hydrogen atom in gelatin peptide bonds and acceptor atoms such as oxygen from free —OH and Si—O—Si groups in MMT. Thus, the FT-IR results indicated that gelatin and CPX–MMT had strong interactions presumably due to the formation of hydrogen bonds between C—H and Si—O—Si. This may be ascribed to the good dispersion of CPX–MMT in gelatin at high CPX–MMT concentrations, which results in larger surfaces of CPX–MMT for interaction with the gelatin molecules.

3.1.2. Thermal analysis

The thermal gravimetric analysis of composite hydrogels was performed to investigate the thermal stability of the composite hydrogel (Fig. 3). TGA patterns of dried MMT were similar to our previous reports [20–24]. The TGA curve of CPX–MMT had three steps for weight loss at the temperatures around 90 °C, 330 °C and 445 °C. One strong and two weak endothermic peaks were observed in DTA patterns. The first weight loss at the temperature around 90 °C was due to free water evaporation from MMT, which was close to our reported drug loading in MMT [20–24,47,48]. The second weight loss with a strong endothermic peak at the temperature around 330 °C was due to the removal of CPX from intercalated MMT. The third endothermic peak due to weight loss at the temperature around 445 °C corresponded to the complete disintegration of CPX–MMT structure. CPX–MMT–gel composite hydrogels were

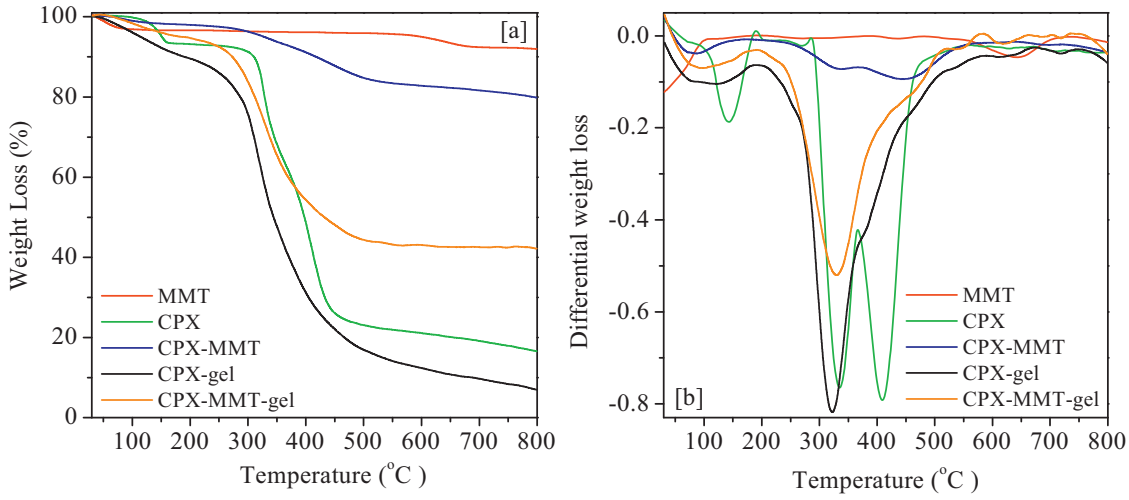

Fig. 3. (a) TGA and (b) DTA pattern.

stable up to 328 °C and revealed four step decomposition behavior. The distinct mass change region was observed over a temperature range of 90–100 °C due to the loss of large amounts of adsorbed water. CPX–MMT–gel composite hydrogels represented moderate decomposition above 328 °C. The complete thermal decomposition of gelatin took place at 545 °C due to the disintegration of amide bonds between gelatin polypeptide chains and hydrogen bond with CPX–MMT. The DSC traces of the CPX–MMT–gel composite hydrogels are shown in supplementary data: S2, with glass transition temperature at 320 °C attributed to intermolecular hydrogen bonding between gelatin and MMT that hinders the flexibility and mobility of gelatin polypeptide chains, supporting the FT-IR results discussed above.

3.1.3. Morphology evaluation by SEM analysis

The SEM images of the pristine MMT, CPX–MMT, CPX–gel and CPX–MMT–gel are shown in Fig. 4. It can be clearly seen that MMT (Fig. 4(a)) had layered structure with platelet morphology consisting of stacked silicate sheets. Fig. 4(b) shows the surface morphology of CPX–MMT hybrid, which revealed slight enlargement of the layered matrix structure due to intercalation of drug between layers of MMT. The SEM image of the CPX–gel hydrogel shows a highly cross-linked structure of interconnected pores (Fig. 4(c)) while, the CPX–MMT–gel composite reveals a large porous matrix with irregular interconnected pore shaped channel like structures with lower interconnection (Fig. 4(d)). It is possible that CPX–MMT particles with higher surface energy will congregate

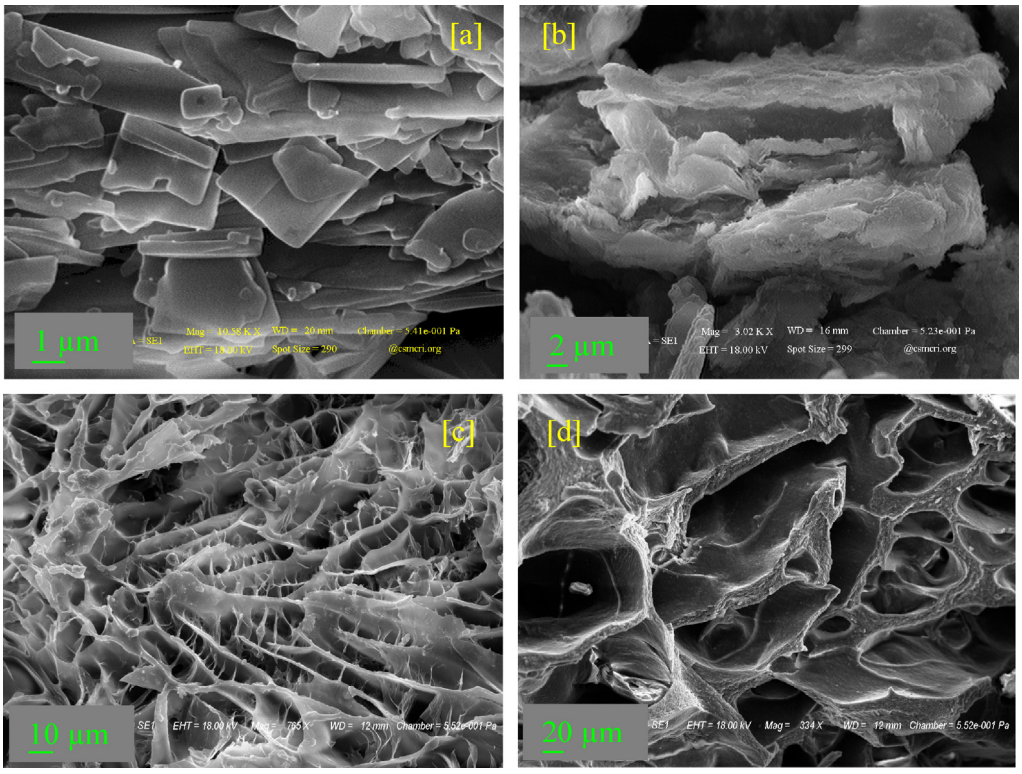

Fig. 4. Surface topology of pristine MMT (a), CPX–MMT hybrid (b), (c) cross-section of CPX–gel and (d) cross-section of CPX–MMT–gel composite hydrogel, imaged by SEM.

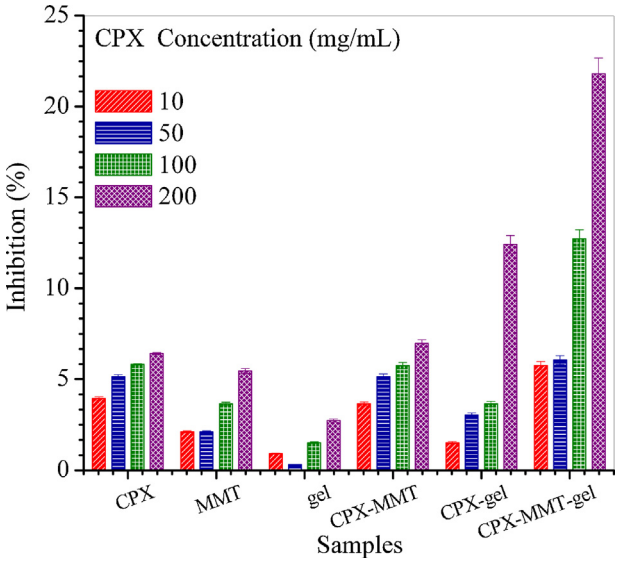

Fig. 5. Inhibition of growth of A549 cells exposed to test compounds measured by MTT assay.

in the gelatin solution when CPX–MMT content is high enough to impact the irregularly interconnected channels.

3.2. MTT assay

A549 are adenocarcinoma human alveolar basal epithelial cell lines, which were developed from a 58-year-old caucasian male [55]. These cells are squamous in nature and carry out diffusion of water and other electrolytes with high potency. Acute lung injury and acute respiratory distress syndrome are of major concerns, where sever irreversible epithelial damage is invoked in the lungs. Wound healing in lung epithelial cells is complex and not much is known about the factors governing [56]. In initial experiments we intended to know about the suitability of matrix in *in vitro* model system.

Fig. 5 shows *in vitro* growth inhibition of A549 cells after exposure to pristine CPX, MMT, gelatin, CPX–MMT, CPX–gel, CPX–MMT–gel composite hydrogels at different concentrations. The CPX–MMT–gel composite hydrogels inhibited maximum growth (~22%) at high dose as compared to pristine CPX and carrier MMT/gelatin materials (~2–6%) in A549 cells. However, exposure of cell cultures to CPX–gel also moderately inhibited cell growth (~12%), which indicated that CPX–MMT–gel composite hydrogels were somewhat detrimental to cells at higher doses. It may be explained by the fact that MMT/gel and intercalated CPX create 3D complex and cover the live cells, leading to deficiency of appropriate nutrition from culture media, hence reducing metabolic activity or blocking transportation of vital molecules to cells [20,21,47,48]. Overall, growth of the cells declined with higher doses of CPX–MMT composite hydrogels as compared to other formulations.

3.3. Effect of CPX–MMT–gel composite hydrogels on A549 cell migration

A549 cells proliferated in the presence of CPX–MMT with gelatin and their migration across the wound edge toward the cell-denuded area increased significantly (ANOVA, $p < 0.05$) (Fig. 6(a) and (b)). Cell densities near the wound edges were also considerably higher than in control and carrier material treated cells, probably due to cell proliferation promoted by gelatin [41–43]. Interestingly, CPX liberation from CPX–MMT–gel composite hydrogels prevented cell culture from contamination and secondly gelatin acted as cell growth promoter or helped cell adhesion to

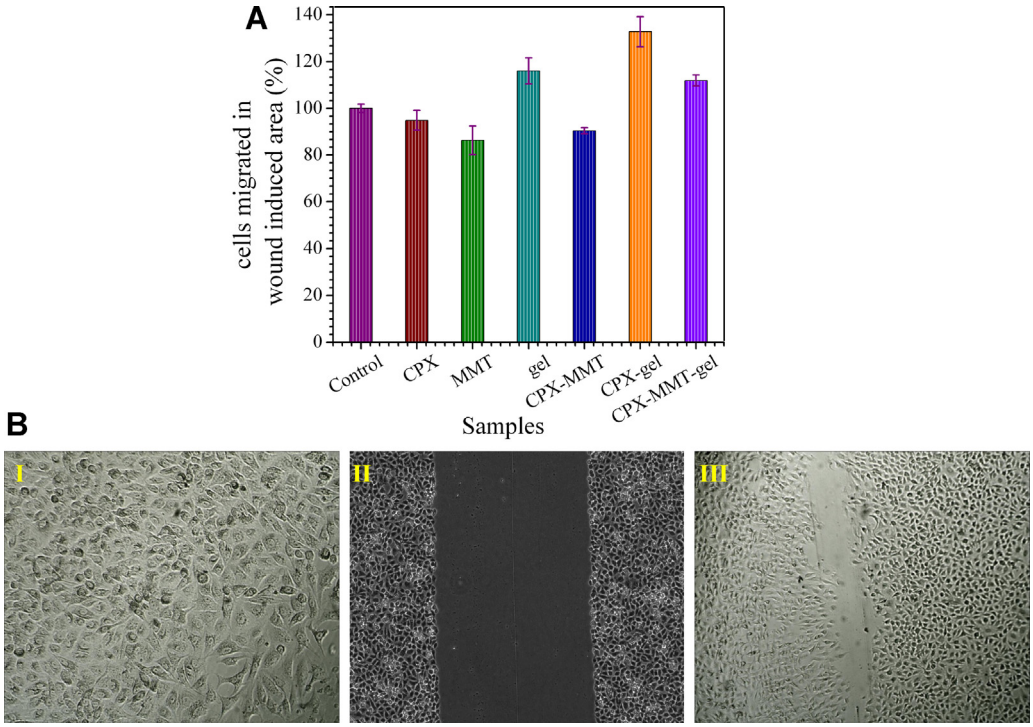

Fig. 6. (a) Quantitative proliferation. (b) Migration assay of A549 cells to carrier materials, CPX–gel, CPX–MMT, MMT and CPX–MMT–gel composite hydrogel. Confluent cell cultures of A549 were wounded with a micropipette tip. The numbers of cells migrated from the edge of the wound within each 250 μm × 500 μm area were counted, data represent mean ± SD ($n = 3$) (significant differences: ANOVA, $p < 0.05$) and (B) positive effect on wound healing and migration of cells. (I) Confluent cells in 12 well culture plate without wound induction, healthy cells serve as control. (II) Cells at "0" h of wound induction showing large vacant space between two cell colonies and (III) cells after 24 h of wound induction and exposure of CPX–MMT–gel composite hydrogels, cells bridge the gap significantly leaving scarce space between the colonies (200×).

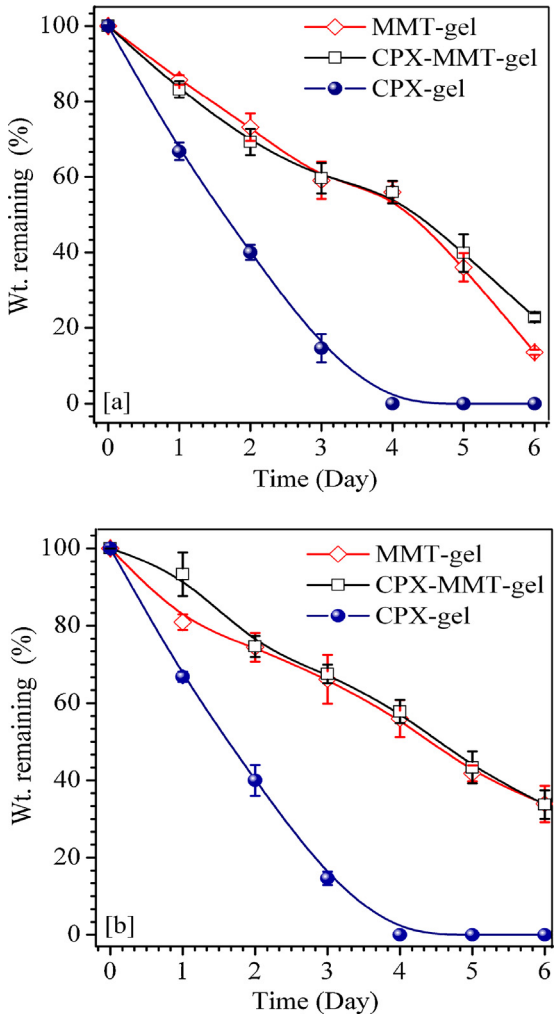

Fig. 7. Effect of proteolytic enzymes on *in vitro* biodegradation of the MMT–gel, CPX–gel and CPX–MMT–gel composite hydrogels: (a) lysozyme and (b) protease K. Data represent mean ± SD ($n = 3$).

the bottom of the flask. Thus, CPX–gel or CPX–MMT–gel composite hydrogels may act as barrier biomaterial against microbes and protect wounds from infection and hence accelerating the healing process.

3.4. In vitro biodegradation behavior

As wound healing aims at regeneration of new cells, the composite hydrogels are expected to be degraded and absorbed with a proper rate to match the speed of new cell formation. The degradation behavior of composite hydrogels in a physiological environment plays an important role in new cell regeneration process. In our work, the *in vitro* biodegradation performance of CPX/gel, MMT–gel and CPX–MMT–gel composite hydrogel in phosphate buffered saline (PBS) containing lysozyme and proteinase K was investigated. The degradation process involves gelatin hydrolyzation by enzymatic degradation [1,57,58]. The effect of lysozyme and proteinase K on the degradation behavior is shown in Fig. 7(a) and (b) where CPX–gel degraded much faster than CPX–MMT–gel or MMT–gel which were preserved due to their 3D structure. The hydrophilic amino and carboxyl groups of gelatin polypeptides can be hydrolyzed by lysozyme and proteinase K. The CPX–gel degraded rapidly because of the large number of hydrophilic amino and carboxyl groups and physical structure of CPX–gel scaffold which had higher porosity and leaner pore-wall.

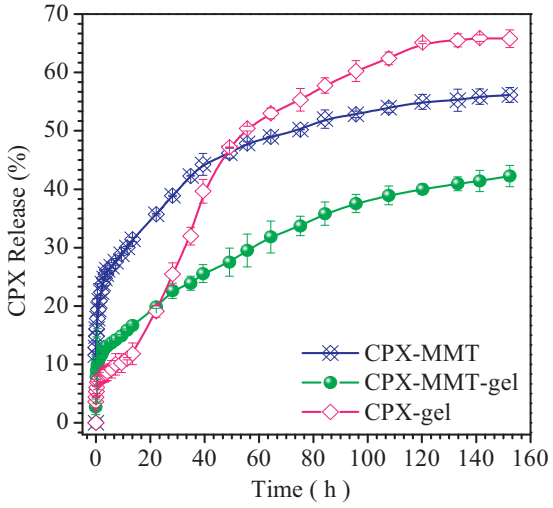

Fig. 8. *In vitro* release patterns of CPX in simulated intestinal fluid (pH 7.4) at 37 ± 0.5 °C; data represent mean ± SD ($n = 3$).

The contact area of gelatin to hydrolyzing enzymes was much larger and the scaffold degraded more rapidly. CPX–MMT–gel and MMT–gel degraded proportionally slowly because of the hydrogen bonding between MMT layers and gelatin polypeptides. It is reasonable to consider that strong interaction between gelatin polypeptide chains, MMT sheets utilized key hydrophilic amino or carboxylic groups depressing water diffusion and protecting gelatin polypeptide chains from hydrolysis. Meanwhile, the presence of MMT also served as physical cross-linking sites, which enhanced the stability of the network. It is anticipated that the free amino and carboxyl groups of gelatin interacted with MMT reducing the water affinity of composite hydrogels and slowing down the rate of degradation. Overall, the phenomena revealed that slow degradation rates of composites might be due to the presence of MMT.

3.5. In vitro drug release study

The release behavior of the CPX from CPX–gel, CPX–MMT hybrid and CPX–MMT–gel composite hydrogels is shown in Fig. 8. CPX from CPX–MMT–gel composite hydrogel showed controlled release pattern with ~26% of drug released in 40 h followed by sustained release up to >150 h (~43%). No initial burst release was observed from CPX–MMT–gel composite hydrogels. The release of the drug from CPX–MMT hybrid was somewhat faster compared to that from CPX–MMT–gel composite hydrogels, where ~24 and 56% of the intercalated drug was released in 6.5 h and 150 h respectively. The drug release from CPX–gel was quicker than CPX–MMT in the initial few hours (0–20 h), a burst release (21–48 h) followed by controlled release. The sustained release of CPX from CPX–MMT–gel composite hydrogels can be attributed to the strong interaction of the CPX–MMT hybrid and gelatin polypeptide chains that lead to formation of 3D structure of composite hydrogel. Eventually, CPX release followed the route of de-intercalation from the MMT layers of gelatin polypeptide chains and release medium. It may also be explained by some structural groups of CPX interacting with gelatin polypeptide chains that lead to slow release of CPX in release medium. The surface charge of MMT is negative [20–24,47,48] which is dissimilar to that of CPX molecules and hence can be easily intercalated into the interlayer space or attached to the surface of MMT due to electrostatic attraction and the path of diffusion from intercalated drug composites from polymeric composites hydrogels were longer. The more general way, drug was sheltered from the aqueous environment for preprogrammed periods of time. This shielding can involve delaying the dissolution of drug molecules,

inhibiting the diffusion of the drug out of the formulation, or controlling the flow of drug solutions [59].

4. Conclusion

We have successfully intercalated CPX into MMT galleries with high drug loading efficiency (35.5% CPX in MMT). Drug loaded in MMT layers had no significant changes in its structural and functional properties. Incorporation of gelatin into CPX–MMT hybrid achieved controlled drug release property and induced cell migration and proliferation. MTT assay revealed that CPX–MMT composites exhibit some cytotoxic effects at high concentration. *In vitro* experiment results showed that composite hydrogels with MMT had slower degradation rate than drug loaded gelatin. It was concluded that the biopolymer and MMT were the key factors for functional properties of composite hydrogels. According to the results obtained, the CPX–MMT–gel composite hydrogels showed excellent biochemical properties which met the essential requirements of ideal biomaterial for tissue engineering. We believe this study will be valuable in designing alternative cost-effective layered silicate composite hydrogels where drug intercalation could lead to prolonged release and find application in designing wound dressing biomaterials for tissue engineering.

Acknowledgments

Authors are thankful to Council of Scientific and Industrial Research (CSIR), Government of India, New Delhi, India, for financial support under the project "Speciality Materials based on Engineered Clays" (SPEC, CSC-0135) and Senior Research Fellowship to Dr. B.D. Kevadiya. Authors are also thankful for help and cooperation rendered by Mr. V. Agarwal (FT-IR) and Mrs. Shital Patel (TGA) of the central analytical facility of CSMCRI.

Appendix A. Supplementary data

Supplementary data associated with this article can be found, in the online version, at http://dx.doi.org/10.1016/j.colsurfb.2014.06.051.

References

[1] J.P. Zheng, C.Z. Wang, X.X. Wang, H.Y. Wang, H. Zhuang, K.D. Yao, React. Funct. Polym. 67 (2007) 780.
[2] A. Vasconcelos, A. Cavaco-Paulo, Appl. Microbiol. Biotechnol. 90 (2011) 445.
[3] R. Sweeney, M. Miraftab, G. Collyer, Int. Wound J. 9 (2012) 601.
[4] S. Pal, Y.K. Tak, J.M. Song, Appl. Environ. Microbiol. 73 (2007) 1712.
[5] M.J. Hajipour, K.M. Fromm, A.A. Ashkarran, D.J. de Aberasturi, I.R. de Larramendi, T. Rojo, V. Serpooshan, W.J. Parak, M. Mahmoudi, Trends Biotechnol. 30 (2012) 499.
[6] A.R. Shahverdi, A. Fakhimi, H.R. Shahverdi, S. Minaian, Nanomedicine 3 (2007) 168.
[7] P. Gong, H. Li, X. He, K. Wang, J. Hu, W. Tan, S. Zhang, X. Yang, Nanotechnology 18 (2007) 285604, http://dx.doi.org/10.1088/0957-4484/18/28/285604.
[8] Z. Xiu, Q. Zhang, H.L. Puppala, V.L. Colvin, P.J.J. Alvarez, Nano Lett. 12 (2012) 4271.
[9] D.A. Talan, K.G. Naber, J. Palou, D. Elkharrat, Int. J. Antimicrob. Agents 23 (2004) 54.
[10] K.S. Abdellaouia, N.V. Castionib, R. Gurny, Eur. J. Pharm. Biopharm. 50 (2000) 83.
[11] V. Mourino, A.R. Boccaccini, J. Roy. Soc. Interface 7 (2010) 209.
[12] K. Kanellakopoulou, M. Kolia, A. Anastassiadis, T. Korakis, E.J. Giamarellos-Bourboulis, A. Andreopoulos, et al., Antimicrob. Agents Chemother. 43 (1999) 714–716.
[13] V. Mathur, R. Mudnaik, L. Barde, A. Roy, U. Shivhare, K. Bhusari, Acta Pharm. 60 (2010) 111.
[14] D. Hesse, M. Badar, A. Bleich, A. Smoczek, S. Glage, M. Kieke, P. Behrens, et al., J. Mater. Sci. Mater. Med. 24 (2013) 129.
[15] B.K. Nanjwade, D.B. Sonaje, F.V. Manvi, Int. J. Novel Drug Deliv. Technol. 1 (2011) 23.
[16] A. Hui, H. Sheardown, L. Jones, Materials 5 (2012) 85.
[17] D. Esrafilzadeh, J.M. Razal, S.E. Moulton, E.M. Stewart, G.G. Wallace, J. Control. Release (2013), http://dx.doi.org/10.1016/j.jconrel.2013.01.022.
[18] T.L. Ke, G. Cagle, B. Schlech, O.J. Lorenzetti, J. Mattern, J. Ocul. Pharmacol. Ther. 17 (2001) 555.
[19] M. Azami, S. Tavakol, A. Samadikuchaksaraei, M.S. Hashjin, N. Baheiraei, M. Kamali, M.R. Nourani, J. Biomater. Sci. 23 (2012) 2353.
[20] B.D. Kevadiya, T.A. Patel, D.D. Jhala, R.P. Thumbar, H. Brahmbhatt, M.P. Pandya, S. Rajkumar, et al., Eur. J. Pharm. Biopharm. 81 (2012) 91.
[21] B.D. Kevadiya, R.P. Thumbar, M.M. Rajput, S. Rajkumar, H. Brambhatt, G.V. Joshi, et al., Eur. J. Pharm. Sci. 47 (2012) 265.
[22] B.D. Kevadiya, G.V. Joshi, H.M. Mody, H.C. Bajaj, Appl. Clay Sci. 52 (2011) 364.
[23] G.V. Joshi, B.D. Kevadiya, H.M. Mody, H.C. Bajaj, J. Polym. Sci. Part A: Polym. Chem. 50 (2012) 423.
[24] G.V. Joshi, B.D. Kevadiya, H.C. Bajaj, Micropor. Mesopor. Mater. 132 (2010) 526.
[25] S.S. Feng, L. Mei, P. Anitha, C.W. Gan, W. Zhou, Biomaterials 30 (2009) 3297.
[26] Y. Dong, S.S. Feng, Biomaterials 26 (2005) 6068.
[27] Q. Yuan, J. Shah, S. Hein, R.D.K. Misra, Acta Biomater. 6 (2010) 1140.
[28] G.V. Joshi, B.D. Kevadiya, H.A. Patel, H.C. Bajaj, R.V. Jasra, Int. J. Pharm. 374 (2009) 53.
[29] D. Depan, A.P. Kumar, R.P. Singh, Acta Biomater. 5 (2009) 93.
[30] M.R. Guilherme, A.R. Fajardo, T.A. Moia, M.H. Kunita, M. do Carmo Goncalves, A.F. Rubira, E.B. Tambourgi, Eur. Polym. J. 46 (2010) 1465.
[31] P.I. Rose, in: H.F. Mark, N.M. Bikales, C.G. Overberger, G. Menges, J.I. Kroschwitz (Eds.), Encyclopedia of Polymer Science and Engineering, Wiley, 1987, pp. 488–513.
[32] P. Johns, A. Courts, in: A.G. Ward, A. Courts (Eds.), The Science and Technology of Gelatin, Academic, London, 1977, p. 138.
[33] A.N. Fraga, R.J.J. Williams, Polymer 26 (1985) 113.
[34] M. Frydrych, C. Wan, R. Stengler, K.U. O' Kelly, B. Chen, J. Mater. Chem. 21 (2011) 9103.
[35] R. Guidoin, D. Marceau, T.J. Rao, M. King, Y. Merhi, P.E. Roy, et al., Biomaterials 8 (1987) 433.
[36] R.A. Jonas, G. Ziemer, F.J. Schoen, L. Britton, A.R. Castaneda, J. Vasc. Surg. 7 (1988) 414.
[37] Y. Marois, N.L. Chakfey, X. Deng, M. Marois, T. How, M.W. King, et al., Biomaterials 16 (1995) 1131.
[38] Y. Tabata, S. Hijikata, Y. Ikada, J. Control. Release 31 (1994) 189.
[39] K. Ulubayram, A.N. Cakar, P. Korkusuz, C. Ertan, N. Hasirci, Biomaterials 22 (2001) 1345.
[40] J.F. Martucci, R.A. Ruseckaite, Polym. Plast. Technol. Eng. 49 (2010) 581.
[41] A.M. Schor, S.L. Schor, T.D. Allen, J. Cell Sci. 62 (1983) 267.
[42] K. Sisson, C. Zhang, M.C. Farach-Carson, D.J.F. Bruce Chase, Rabolt, J. Biomed. Mater. Res. Part A 94A (2010) 1312.
[43] T.C. Lim, W.S. Toh, L.S. Wang, M. Kurisawa, M. Spector, Biomaterials 33 (2012) 3446.
[44] T. Mosman, J. Immunol. Methods 65 (1983) 55.
[45] L.G. Rodriguez, X. Wu, J.L. Guan, Meth. Mol. Biol. 294 (2005) 23.
[46] A. Khan, I. Zafar, A.K. Jamshaid, S.K. Ghulam, M. Bilal, T.M. Khan, Arch. Pharm. Pract. 2 (2011) 116.
[47] B.D. Kevadiya, S.S. Chettiar, S. Rajkumar, H.C. Bajaj, K.A. Gosai, H. Brahmbhatt, Colloids Surf. B: Biointer. 112 (2013) 400.
[48] B.D. Kevadiya, S.S. Chettiar, S. Rajkumar, H.C. Bajaj, H. Brahmbhatt, J.C. Chaudhari, R.P. Thumbar, D. Jhala, M.V. Rao, Compos. Sci. Technol. 90 (2014) 193.
[49] S. Pisal, R. Zainnuddin, N. Pradeep, K. Mahadik, Kadam S, AAPS Pharm. Sci. Technol. 5 (2004) 62.
[50] R.H. Clarke, S. Londhe, W.R. Premasiri, M.E. Womble, J. Raman Spectrosc. 30 (1999) 827.
[51] R.M. Silverstein, F.X. Webster, Spectrometric Identification of Organic Compounds, 6th ed., John Wiley and Sons, New York, 2002.
[52] R.T. Tom, V. Suryanarayana, P.G. Reddy, S. Baskaran, T. Pradeep, Langmuir 20 (2004) 1909.
[53] M.C. Chang, C.C. Ko, W.H. Douglas, Biomaterials 24 (2003) 2853.
[54] A. Sionkowska, M. Wisniewski, J. Skopinska, C.J. Kennedy, T.J. Wess, Biomaterials 25 (2004) 795.
[55] D.J. Giard, S.A. Aaronson, G.J. Todaro, P. Arnstein, J.H. Kersey, H. Dosik, W.P. Parks, J. Nat. Cancer Inst. 51 (5) (1973) 1417.
[56] T. Geiser, M. Ishigaki, C. Leer, M. Matthay, AJP: Lung Physiol. 287 (2) (2004) 448.
[57] T. Chen, D.A. Small, M.K. McDermott, W.E. Bentley, G.F. Payne, Biomacromolecules 4 (2003) 1558.
[58] Y. Huang, S. Onyeri, M. Siewe, A. Moshfeghian, S.V. Madihally, Biomaterials 26 (2005) 7616.
[59] K.E. Uhrich, S.M. Cannizzaro, R.S. Langer, K.M. Shakesheff, Chem. Rev. 99 (1999) 3181.